

Quantum interference in dirty d -wave superconductors

Hong-Yi Chen*, Lingyin Zhu†, and C.S. Ting*

*Texas Center for Superconductivity and Department of Physics, University of Houston, Houston, TX 77204

†Department of Physics, State University of New York at Buffalo, Buffalo, NY, 14260

The local differential tunneling conductance on a Zn impurity in a disordered d -wave superconductors is studied. Quantum interference between many impurities leads to definitive quasiparticle spectra. We suggest that an elaborate analysis on impurity-induced spectra with quantum interference effect included may be able to pin down the sign and strength of the scattering potential of a Zn impurity in low density limit. Numerical simulations calculated with appropriately determined impurity parameters are in satisfactory agreement with the observations from scanning tunneling microscopy (STM) experiments even in subtle details.

PACS numbers: 74.25.Jb, 74.20.-z, 74.50.+r

Impurity effect has served as a unique probe to the mechanism of unconventional superconductivity. Recently, remarkable improvements in high resolution STM experiments provided unprecedently delicate images of electronic structure around doped Zn in $\text{Bi}_2\text{Sr}_2\text{CaCu}_2\text{O}_{8+\delta}$ (BSCCO)¹. The defect states in differential conductance map at low temperatures bear on almost identical spectroscopic and spatial structures from one impurity to the other, with characteristic on-site zero bias resonance peak, four-fold symmetry pattern in local density of states (LDOS) and locally suppressed superconductivity at immediate surroundings of Zn atoms. These observations are in qualitative agreement with preceding theoretical works which model Zn atoms as isolated pointlike unitary centers embedded in a superconducting background of d -wave like pairing symmetry^{2,3}. However, although the single-impurity scenario (SI) is approximately successful in interpreting the energy and spatial symmetry of resonant states, it fails to reproduce the subtle features in the spatial profile of LDOS extracted by STM measurements. Attempts to reconcile this discrepancy include postulations on the tunneling matrix of STM probes^{4,5}, possible Kondo physics from staggered moment⁶ and etc.; nevertheless, the determination of the attributes of Zn impurities, with which we can substantiate reliable calculations to compare with experiments, remains divergent itself: even assuming Zn impurities are purely potential scatterers, one could still reach completely opposite conclusions that they are either repulsive (as desired to yield unitary limit with realistic cuprates band) or attractive (*relative to the background Cu ions*) according to their ionic configuration. Most recently, an *ab-initio* calculation based on density functional theory concludes that Zn should be repulsive centers to electrons⁷.

In the meanwhile, the effect of *interference* between the quasiparticle resonances cannot be neglected. Overlapping between disorder-induced Fridel oscillations alters local landscape in LDOS and populates the low energy excitations, which greatly modify the spectroscopic and transport properties of cuprates. There have been numerous theoretical studies on many-impurity problem^{8,9,10,11,12,13}, with emphasis either on the effect

of impurity network on Fourier transformed power spectrum which can be used to extract the kinematics of pure systems or on the asymptotic behavior of Fermi level density of quasiparticle states. Despite the creditable achievements of these endeavor in interpreting STM data, the lingering unjustification of impurity parameters could place their arguments on a shaky ground; moreover, none of them have given full attention to the potential of combining interference effect to discuss the impurity spectra and identify the impurity characteristics itself. It is then the purpose of this paper to argue that through elaborate investigation on quantum interference effect in a fully disordered system, we could nail the identities of Zn impurity such as its sign and strength and hopefully close the debate on this issue to our best.

We start by writing down the generic many-impurity Hamiltonian as,

$$H_{Zn} = \sum_{i\sigma} \phi(r_i) c_{i\sigma}^\dagger c_{i\sigma} , \quad (1)$$

where $c_{i\sigma}^\dagger (c_{i\sigma})$ creates (annihilates) an electron with spin σ at site r_i and $\phi(r_i)$ is the impurity strength on the perturbed site. Randomness of impurity distribution makes counting relative coordinates information between all the impurities a formidable task. Therefore a systematic and reliable manipulation of the interference, yet not losing the reality and generality, will be helpful. We tacitly suggest to fix the first impurity at the center ($r = 0$) of the lattice and keep injecting others while requiring that the inter-impurity distance of any pair, i.e., $R_{ij} = |r_i - r_j|$ has to be greater than a preset cutoff d_0 . This constraint excludes the possibility of cluster formation and further guarantees a uniform distribution of disordered sites. The central impurity, which is the focus of our discussion later, is believed to be the representative of a arbitrary one surrounded by other disordered sites that are randomly distributed in real samples. Therefore, a single parameter, i.e., the concentration, will be the defining parameter instead of the relative orientation and distance between impurities. The effect of the quantum interference is then parameterized as a function of the concentration x (or the number of impurities N_{imp}) in a fixed

lattice size.

We study this problem using the conventional Bogoliubov-de Gennes' (BdG) formalism:

$$\sum_j^N \begin{pmatrix} \mathcal{H}_{ij} & \Delta_{ij} \\ \Delta_{ij}^* & -\mathcal{H}_{ij}^* \end{pmatrix} \begin{pmatrix} u_j^n \\ v_j^n \end{pmatrix} = E_n \begin{pmatrix} u_i^n \\ v_i^n \end{pmatrix}, \quad (2)$$

where $\mathcal{H}_{ij} = -t_{ij} + (\phi(r_i) - \mu) \delta_{ij}$ is the single particle Hamiltonian, t_{ij} is the hopping integral, μ is the chemical potential, $\Delta_{ij} = \frac{V}{2} (c_{i\uparrow} c_{j\downarrow} - c_{i\downarrow} c_{j\uparrow})$ is the spin-singlet bond order parameter, V is the nearest-neighbor attractive potential, u_i^n and v_i^n are the eigenfunctions of the BdG equations, and E_n is the eigen-energy. The self-consistent conditions are applied to solve the BdG equations:

$$\langle n_{i\uparrow} \rangle = \sum_{n=1}^N |u_i^n|^2 f(E_n), \quad (3)$$

$$\langle n_{i\downarrow} \rangle = \sum_{n=1}^N |v_i^n|^2 [1 - f(E_n)], \quad (4)$$

$$\Delta_{ij} = \sum_{n=1}^N \frac{V}{4} (u_i^n v_j^{n*} + v_i^{n*} u_j^n) \tanh\left(\frac{\beta E_n}{2}\right), \quad (5)$$

where $f(E) = 1/(e^{\beta E} + 1)$ is the Fermi distribution. We use the following parameters throughout this paper: $\langle t_{ij} \rangle = t = 150$ meV, $\langle t_{ij} \rangle = t' = -0.3t$, $V = 1t$. This prepares us a hole-like Fermi surface with the hole doping $1 - n_f = 1 - \sum_{i\sigma} \langle c_{i\sigma}^\dagger c_{i\sigma} \rangle / N_x N_y = 0.15$, i.e., optimally doped region and a maximum gap magnitude about 45 meV. The local density of states takes the following expression:

$$\rho_i(E) = -\frac{2}{M_x M_y} \sum_{n\mathbf{k}}^N \left[|u_i^{n\mathbf{k}}|^2 f'(E_{n,\mathbf{k}} - E) + |v_i^{n\mathbf{k}}|^2 f'(E_{n,\mathbf{k}} + E) \right], \quad (6)$$

where the factor of 2 arises from spin degeneracy. The summation in $\rho_i(E)$ is averaged over $M_x \times M_y$ (in our paper 20×20) wavevectors in the first Brillouin zone.

Single impurity We start our discussion with a brief review on the single impurity model and plot the resulting spectra in Fig.1 with the “blocking effect” (which is addressed below) included. We unbiasedly picked up a repulsive potential $\phi = 3.0$ eV. Because of the Bogoliubov symmetry of quasiparticles, the on-site LDTC is expected to display two resonance peaks at $\Omega_0^\pm = \pm 0.015t^2$ [see Fig.1(a),(b)]. While the spatial scale and symmetry of impurity states observed in STM fit well with the prediction of SI theory, the relative spectral weight distribution is completely reverted^{3,8}: experimental images at $\Omega = -1.5$ meV¹ displays an on-site maximum spectral intensity, a local minimum on its nearest neighbor sites and a second maximum on the next nearest sites, as illustrated schematically in Fig.1(d). This inconsistency gave

birth to the conjectures regarding the indirect tunneling through the insulating BiO layer: the “filter effect” due to the coherent tunneling⁵ and an alternative “blocking effect” due to the incoherent tunneling¹⁴. In our paper, we will stick to the argument of the latter, in which the “local differential tunneling conductance (LDTC)” fetched by STM probes is believed to measure acutally the averaged LDOS over the four nearest neighbor sites, i.e.,

$$G_i(E) = \frac{1}{4} \sum_{\hat{\mathbf{e}}} \rho_{i+\hat{\mathbf{e}}}(E), \quad (7)$$

where $\hat{\mathbf{e}}$ is $\pm\hat{x}$ or $\pm\hat{y}$. Fig 1.(a),(b),(c) are then plotted with the “blocking effect” included intentionally. In Fig.1(c), the spatial distribution of spectral intensity mimics experimental results under this manipulation. However, corresponding on-site spectra [Fig 1(a)] deviates from the result of Pan *et al.* remarkably: the former shows a sharp peak with excess spectral background at negative bias and a second resonance at positive side; the latter displays a zero bias conductance peak and a second small peak on negative bias; furthermore, Pan *et al.* showed that the Friedel oscillation along the nodal direction decays surprisingly faster than that of the antinodal direction. This is rather counterintuitive since the subgap resonances in *d*-wave superconductors overlap with the vanishing continuum and hence are virtually bounded, with supposedly extended tails along the nodal direction due to the vanishing order parameter. We argue that with the inclusion of quantum interference effect, all this discrepancy will be reconciled provided that the impurity parameter is properly settled.

Many impurity We investigate the quantum interference effect by embedding 10 impurities in an otherwise clean lattice, which yields $x = 0.41\%$, close to laboratory terms. The lattice size is of $N_x \times N_y = 49 \times 49$. Fig. 2 enumerates the on-site LDTC for different values of impurity strength systematically. Generally, quantum interference splits the single impurity resonances into multiple peaks, as illustrated in Fig. 2 and extracting distinctive information from those peaks directly is not easy. However, the zero energy residual LDOS $\rho(\omega = 0)$ is particularly useful as it evolves systematically with respect to the impurity potential. When $\phi = -3.0$ eV, $\rho(\omega = 0)$ is considerably large; as ϕ increases but remains negative (*attractive*), $\rho(\omega = 0)$ decreases until it is completely depleted. This tendency can be understood qualitatively in the sense that the sample recovers its clean spectra which has vanishing $\rho(\omega = 0)$ when less contaminated. When ϕ becomes positive and increases (*repulsive*), $\rho(\omega = 0)$ aggregates remarkably and multiple peaks merge into a “single resonance peak” when ϕ is around the value with which unitary limit is obtained in single impurity analysis. Fig. 2(d) shows such a strong resonance peak at negative bias slightly below zero, whose width and height are in fair agreement with the result of Pan *et al.*. The likeness between Fig. 1(a) and Fig. 2(d) will plausibly suggests the single-impurity physics as dominating mech-

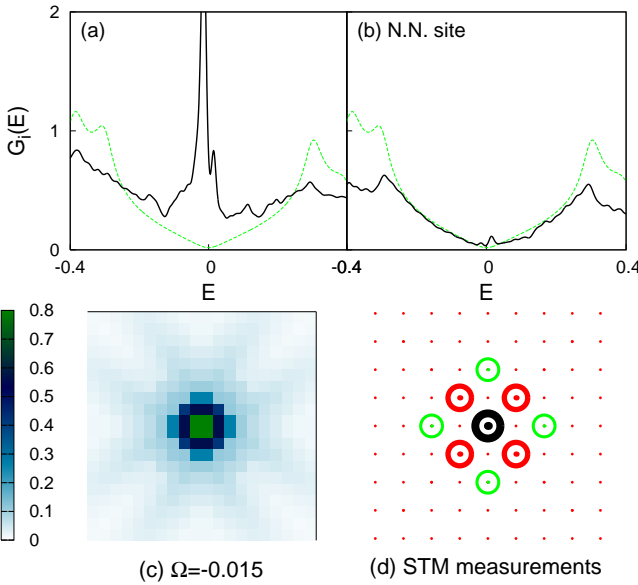


FIG. 1: (a) LDTC on the impurity-site. Dashed green: pure system; solid black: LDTC with the present of single impurity; (b) LDTC on the nearest neighbor site. Dashed green: pure system; solid black: LDTC with the present of single impurity; (c) calculation on spatial distribution of LDTC at $\Omega_0 = -0.015t$; impurity site is placed at the center of the squared window. (d) Schematic plot of the STM image of one impurity¹.

anism and the fact that Zn impurities in the experimental conductance maps appear to be isolated entities with nearly undisturbed four-fold symmetry in LDTC seemingly supports this viewpoint. However, it is worthwhile to point out that exact width of this zero-bias resonance in Fig. 2(d) and STM experiments¹ is ~ 10 meV, an order of magnitude bigger than what single-impurity theory expects but agrees well with the impurity bandwidth in unitarity low density limit, i.e., $\gamma = \sqrt{n_i \Delta_0 E_F}$ ¹⁵. Hence the figurative resemblance between the on-site LDTC's of many-impurity and single-impurity must be the consequence of quantum interference between dilute impurity states and the "homogeneous broadening" effect which was proposed by Atkinson *et al.*¹³ and is not negligible in laboratory terms. The possibility of $|\phi|$ being weak (less than 0.4 eV) is excluded, as it will not introduce any prominent resonant behavior and observable interference effect requires inter-impurity distance as close as $3a$, corresponding to an unreasonably large population of disordered sites. This is demonstrated in Fig. 2(e) and 2(f): when $\phi = \pm 0.3$ eV, the on-site LDTC of dirty samples are essentially coincident with that of single-impurity case. Collection of all the facts above and comparison with experiments lead us to believe that Zn atoms in BSCCO-2212 be *repulsive* potentials at least in the zeroth order.

The exact magnitude of Zinc impurity is still open to determination, but favorably it should not differ too much from the value which approximates single-impurity

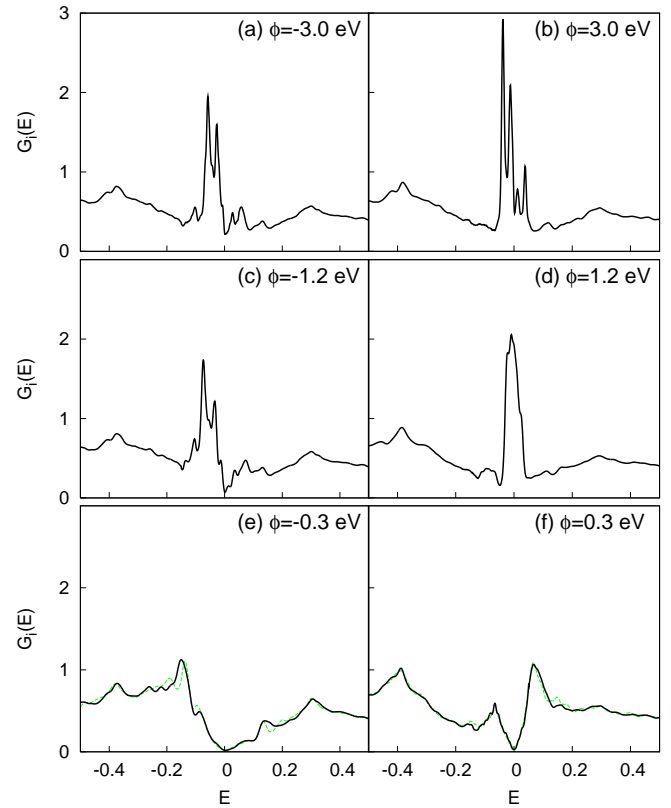


FIG. 2: The local differential tunneling conductance (LDTC) on the central Zn impurity with 10 impurities embedded in the lattice. Left panel: negative potentials (a) -3.0 eV (c) -1.2 eV (e) -0.3 eV. Right panel: positive potentials (b) 3.0 eV (d) 1.2 eV (f) 0.3 eV. Green curves in (e) and (f) are on-site LDTC of single-impurity case.

unitary limit (which is $\phi = 1.2$ eV here) with the cuprates band structure since the unitary scattering due to doped Zn is verified by the scattering phase shift of 0.49π in experiments¹. We then adopted $\phi = 1.2$ eV as the input of calculations and the results are plotted in Fig. 3. The spectrum in channel (a) shows a striking agreement with the result of Pan *et al.* with a sharp resonant peak forming at $\Omega = 0$ and a second smaller peak on negative bias. Apparently, single-impurity scattering fails to interpret both the asymmetry of the peaks positions and the broadened peak widths. While the staggered magnetic interaction may also address the two-peak structure, we would rather believe that the negative peak should arise collectively from inter-impurity correlations and our numerical inspection confirms that it actually persists in a fairly wide region of positive ϕ 's; in Fig. 3(b), the spatial distribution of the resonance around a Zn impurity shows the local minima of the four nearest-neighbor sites, and the local maxima of the eight 2nd-nearest- and 3rd-nearest-neighbor sites clearly forming a "box" around this Zn atom; in Fig. 3(c), the normalized LDTC $G(\mathbf{r})$ at resonance frequency is plotted as a function of distance away from the impurity along the nodal and antinodal directions. The strength of the normalized

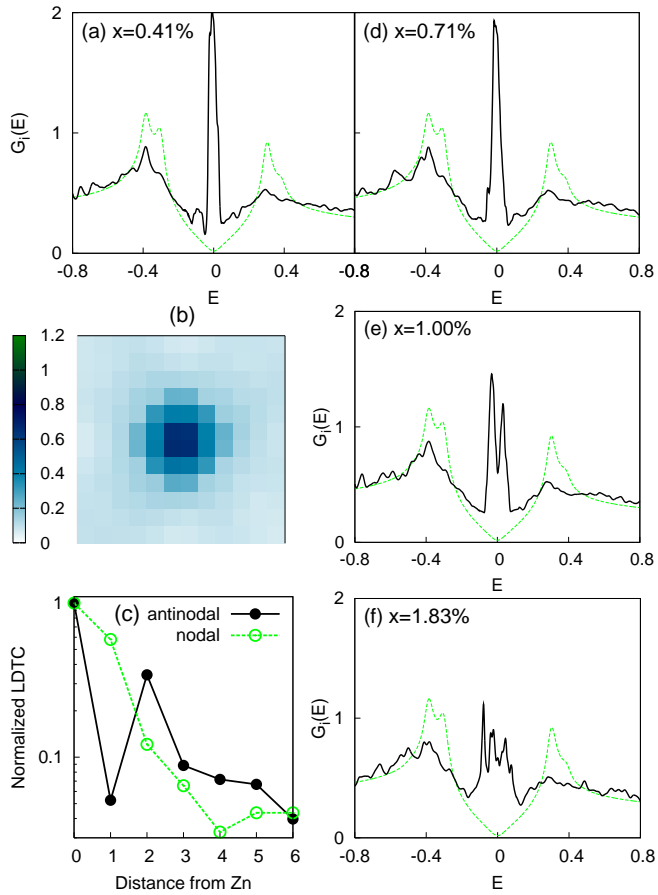


FIG. 3: (a) The LDTC $G_i(E)$ on a Zn impurity at $r = 0$ for $x = 0.42\%$. The dashed line represents the LDTC far away from Zn impurities; (b) The spatial profile of LDTC maps at $\Omega = -2.4$ meV; (c) The LDTC (normalized to the peak value) versus distance from the Zn impurity; (d)(e)(f) The LDTC $G_i(E)$ on the Zn impurity at $r = 0$ for $x = 0.75\%, 1.0\%, 1.83\%$.

LDTC in the nodal direction is found to decay faster than that along the antinodal direction, reinforcing what is ob-

served in STM experiments¹. All this above agree with STM observations remarkably and are confirmed to be robust against the change of ϕ within a wide range centered at 1.2eV; When impurity concentration increases, the low energy excitations are further populated and a subgap impurity band is established gradually, which will suppress superconductivity eventually and is referred to as “impurity band”, in analogy to similar phenomena in semiconductors. This is illustrated schematically in Fig. 3(d)(e)(f), where the zero bias impurity resonance is further broadened and finally into multiple-peak structure with excessive spectral weight filling up the gap region when impurity concentration is several times bigger than the experimental value (0.2% – 0.5%).

Conclusion: We discuss how quantum interference between many impurities can produce qualitatively different spectral features when the impurity variables change. With a numerical study on the disorder induced local spectra (on impurity site), we would like to close the debate over the identity of Zn impurity by concluding that Zn atoms in $\text{Bi}_2\text{Sr}_2\text{CaCu}_2\text{O}_{8+\delta}$ are *repulsive* to electrons in nature with a strength close to unitary limit provided that other internal degrees of freedom was not considered. The discrepancy between STM experiments and the results of single-impurity analysis can be reconciled satisfactorily by taking the quantum interference and insulating layer blocking effect into consideration simultaneously. Our numerical calculations with impurity parameter determined in this paper match STM experiments up to subtle details. We then would emphasize that the results obtained in laboratories should actually be interpreted within the frame of collective quantum interference processes rather than the single impurity physics.

Acknowledgements: We thank S.H. Pan, J.X. Zhu, J. O’Neal, Ang Li and P.J. Hirschfeld for stimulating comments and suggestions. This work is supported by the Texas Center for Superconductivity at the University of Houston, and by a grant from the Robert A. Welch Foundation under No. E-1146.

¹ S.H. Pan, E.W. Hudson, K.M. Lang, H. Eisaki, S. Uchida, and J.C. Davis, *Nature* **403**, 746 (2000).

² A.V. Balatsky, M.I. Salkola, and A. Rosengren, *Phys. Rev. B* **51**, 15547 (1995).

³ A.V. Balatsky, I. Vekhter, and Jian-Xin Zhu, [cond-mat/0411318](http://arxiv.org/abs/cond-mat/0411318).

⁴ J.X. Zhu and C.S. Ting, *Phys. Rev. B* **64**, 060501(R) (2001).

⁵ I. Martin, A.V. Balatsky, and J. Zaanen, *Phys. Rev. Lett.* **88**, 097003 (2002).

⁶ A. Polkovnikov, S. Sachdev, and M. Vojta, *Phys. Rev. Lett.* **86**, 296-299 (2001).

⁷ L.-L. Wang, P.J. Hirschfeld and Haiping Chen, [cond-mat/0505014](http://arxiv.org/abs/cond-mat/0505014).

⁸ Lingyin Zhu, W.A. Atkinson, and P.J. Hirschfeld, *Phys.*

Rev. B **67**, 094508 (2003).

⁹ Y. Onishi, Y. Ohashi, Y. Shingaki, and K. Miyake, *J. Phys. Soc. Jpn.* **65**, 675 (1996).

¹⁰ C. Pepin and P.A. Lee, *Phys. Rev. B* **63** 054502 (2001).

¹¹ D.K. Morr and N.A. Stavropoulos, *Phys. Rev. B* **66**, 140508(R) (2002).

¹² Brian Møller Andersen and Per Hedegård, *Phys. Rev. B* **67**, 172505 (2003)

¹³ W.A. Atkinson, P.J. Hirschfeld and Lingyin Zhu, *Phys. Rev. B*, **68**, 054501 (2003).

¹⁴ J.X. Zhu, C.S. Ting, and C.R. Hu, *Phys. Rev. B* **62**, 6027 (2000).

¹⁵ The unitary low density limit is obtained by *neglecting* quantum interference effect in self-consistent *T*-matrix approximation. However, it gives the impurity band width

with the right order of magnitude.